Asymmetric and symmetric Wulff constructions of islands shapes on a missing-row reconstructed surface

Albada, S.B. van; Rost, M.J.; Frenken, J.W.M.

Asymmetric and symmetric Wulff constructions of island shapes on a missing-row reconstructed surface

S. B. van Albada, M. J. Rost, and J. W. M. Frenken
Kamerlingh Onnes Laboratory, Leiden University, P.O. Box 9504, 2300 RA Leiden, The Netherlands
(Received 7 July 2001; revised manuscript received 15 February 2002; published 22 May 2002)

The two-dimensional equilibrium shapes and structures of adatom or vacancy islands on the (1×2) missing-row (MR) reconstructed Au(110) surface have special characteristics. One type of island has steps parallel to the MR's on opposite sides of the island, which differ both in structure and in formation energy. Hence, the polar step free-energy plot is asymmetric with respect to the Wulff point, and one also expects an asymmetric island contour via the Wulff construction. However, the equilibrium shape of these islands *does* appear to be symmetric. We show that the Wulff point and the island center do not necessarily coincide and explain how a symmetric equilibrium shape can result from an asymmetric Wulff plot. A second island type has identical steps on opposite sides, which are curved into an almond shape with sharp corners. The Wulff constructions of both types of islands are calculated analytically, and the temperature dependence of the contour shapes is investigated. The results are confirmed by Monte Carlo simulations.

DOI: 10.1103/PhysRevB.65.205421 PACS number(s): 68.35.Md, 05.70.Np, 05.50.+q

I. INTRODUCTION AND OUTLINE

The equilibrium shape of a two-dimensional (vacancy) island on a flat crystal surface can be constructed from the polar plot of the step free energy $f(\phi)$ by applying the two-dimensional version of the well-known Wulff construction.[1,2] As an example, Fig. 1 shows the construction for the case of Cu(110) at 400 K. To every point of the polar plot, a line segment is drawn from the origin W (Wulff point), such as the one in the upper left quadrant. At the end point of this line segment, a perpendicular line is constructed. When all the latter lines are combined, as in the upper right quadrant, the interior contour has the shape which minimizes the total free energy of the island for a fixed total island area. This graphical construction is equivalent to applying a Legendre transform to the polar free energy plot.[4,5]

A popular method to determine ratios between step free energies is to apply the inverse Wulff construction to images of two-dimensional islands. One identifies the Wulff point as the center of mass of an island and then applies the Wulff construction in reverse order to obtain the step free-energy plot to within a constant scale factor.[6,7] In addition, the temperature dependence of the island shape can be used to obtain an absolute scale for the step free energies.[8]

In Secs. II and III of the current paper we show that the inverse Wulff construction cannot always be performed. In some cases the Wulff point W does not coincide with the center of the island. This peculiar situation can occur for islands on a *reconstructed* surface, such as Au(110) (1×2) and Pt(110) (1×2). In general, in the Wulff construction of any one-, two-, or three-dimensional structure with a broken symmetry, the Wulff point falls outside the structure's center. In Sec. IV we develop a method to calculate free energies of steps on a missing-row reconstructed surface. We apply this method to the two-dimensional Ising model and to two different approximations. In Sec. V the equilibrium shapes of two types of island on Au(110) as a function of temperature are determined via Wulff constructions, and results of the three models are compared to results of Monte Carlo simulations. Finally, some more exceptional characteristics of the islands are explained, such as the presence of cusplike maxima in the free-energy plot and of sharp corners in the equilibrium shape at nonzero temperature and the diverging of the aspect ratio.

II. ISLANDS ON AU(110)

Figure 2(a) is a sphere model of the Au(110) surface seen from above. It shows the (1×2) missing-row reconstruction (MRR): every second atom row along the $[1\bar{1}0]$ direction is missing. As a consequence, the distance along the [001] direction between two atom rows, which we will call the MRR period, is doubled to $2\sqrt{2}$ times the interatomic distance along the $[1\bar{1}0]$ direction. Also shown in Fig. 2(a) is a vacancy island of one monolayer deep. Such islands can be made by mild sputtering of a flat Au(110) surface.[9] Scanning tunneling microscopy (STM) on the sputtered surface has shown that MRR is present inside all vacancy islands. MRR is found even within the smallest vacancy islands of just one atom row wide.[9] The vacancy island in Fig. 2(a) has a width of four MRR periods. MRR forces the island to adopt an asymmetric internal structure: the four atom rows inside the island could equally likely be placed one-half MRR period to the right. Figure 2(b) shows a cross section of the island along AB. The left and right steps are different in structure. We call the one on the left a (331) step, because a sequence of these steps would form a Au(331) surface; for the same reason, we call the one on the right a (111) step. In Fig. 2(a) the structures of the kinks that occur in the two steps can be seen, which we will call (331) and (111) kinks. The creation energy of a kink can be split into two contributions:[10] the energy of the added step segment and the corner energy, defined as the sum of the energies of the kink's convex and concave corners. A (331) and a (111) kink both contain a

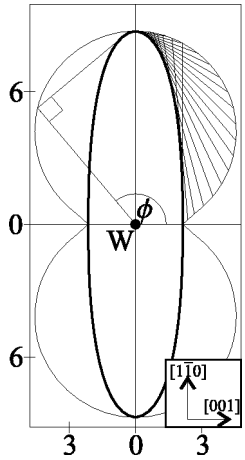

FIG. 1. Polar plot of the free energy $f(\phi)$ of steps on Cu(110) at 400 K (thin curve). Energies are expressed in meV/Å. The Wulff construction is used to determine the equilibrium shape of islands on this surface (thick curve). The step free energy at each angle ϕ has been calculated under the assumption that the formation energy for each step configuration is a simple sum of formation energies of atomic step segments along the two symmetry directions [001] and [1$\bar{1}$0]. For these we used values of $\epsilon_{[001]}=102$ meV per lattice spacing along [001], of 3.61 Å, and $\epsilon_{[1\bar{1}0]}=9$ meV per lattice spacing along [1$\bar{1}$0], of 2.55 Å, obtained from effective-medium-theory calculations Ref. 3. The directions of the [1$\bar{1}$0] and [001] steps are indicated by the arrows.

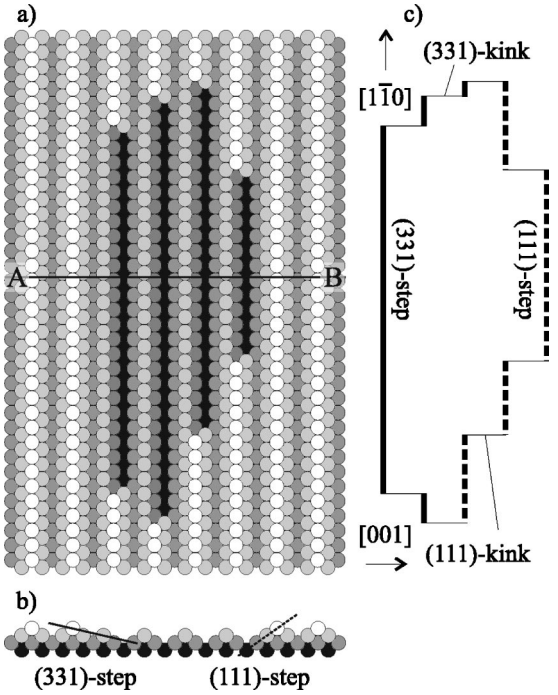

FIG. 2. (a) Sphere model of a vacancy island in the (1×2) reconstructed Au(110) surface. (b) Cross section along AB. As a consequence of the missing-row reconstruction inside and outside the vacancy island, the steps at the left and right sides of the vacancy island are different. (c) Schematic top view of the island contour. The (331) steps are indicated with solid lines and the (111) steps with dashed lines.

[001]-step segment, with two broken atomic bonds in the [1$\bar{1}$0] direction, but the corners have different structures. In the schematic top view of the vacancy island of Fig. 2(c), the different types of steps and kinks are indicated: the solid lines represent (331) steps and the dashed lines (111) steps. The (111) step has a denser packing than the (331) step [Fig. 2(b)], and its formation energy is substantially lower.[11] Therefore, we may expect that also the free energy of a (111) step is lower than that of a (331) step. Thus, in the polar free-energy plot, the distance from the Wulff point to the (111) step (free energy) will be shorter than the distance to the (331) step (free energy). This possibility of a Wulff construction with different free energies for opposite step directions was mentioned before by Van Beijeren and Nolden.[12] The consequence for the case of Au(110) is that the Wulff plot cannot have mirror symmetry with respect to the [1$\bar{1}$0] axis through the Wulff point. If we apply the Wulff construction, we can never obtain an average island contour that is symmetric with respect to this axis, and one may therefore expect to find an asymmetric island shape.

III. SYMMETRY OF THE ISLAND

When the step free energy is different for two different step orientations, the island shape usually reflects this, with the lower-energy step orientation represented more prominently than the other one. Therefore, we might naively expect to find more of the (111) step than of the (331) step in the vacancy islands on Au(110). This, however, is impossible, because the left and right sides of an island simply must have the same length. This means that the islands cannot adopt an asymmetric contour as a consequence of the difference in the energies of (111) steps and (331) steps (from here on, we will use the word ''symmetry'' to indicate mirror symmetry with respect to the [1$\bar{1}$0] direction). The only way for the island to break its symmetry is to have more kinks on one side of the island than on the other (Fig. 3). This can happen as the consequence of a difference in kink energies. If, for example, the formation energy of a (331) kink, $\epsilon_{kink(331)}$, were lower than that of a (111) kink, $\epsilon_{kink(111)}$, each island would on average contain more (331) kinks, making shapes like the one in Fig. 3(a) more favorable than shapes like in Fig. 3(b). In this case, the average island shape would be more rounded on the (331) side and straighter on the (111) side.

The STM experiments performed in Ref. 9 show that the average island shape is symmetric. Both types of kink appear with the same frequency. From the numbers of kinks counted in the images, the two kink energies were calculated to be equal within 1.2 meV, which is 6 permille of the total kink energy. Of course, asymmetric island shapes like Fig. 3(a) do occur, but their mirror images [Fig. 3(b)] occur with precisely the same frequency, because the two shapes have the same formation energy. It is the *average* island shape, which is symmetric.[13]

Still, the polar free-energy plot is asymmetric. How can an *asymmetric* polar-step free-energy plot produce a *symmetric* island contour? This counterintuitive situation is illus-

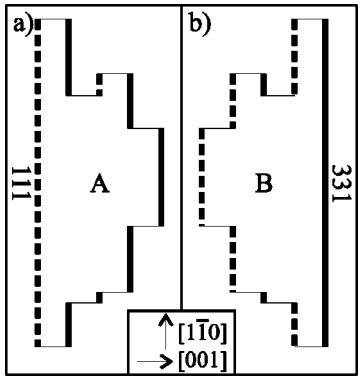

FIG. 3. In each of the two mirrored vacancy islands in (a) and (b) the total length of the (331) step is identical to the total length of the (111) step. Therefore, the total energies of the $[1\bar{1}0]$-oriented parts of the steps of islands *A* and *B* are equal. If the energies of (331) and (111) kinks are equal, the two islands have the same total formation energy. In that case, every island shape will occur with the same frequency as its mirror image and the average island contour will be symmetric.

trated in Fig. 4. The Wulff construction in Fig. 4 has some remarkable characteristics. The construction is very asymmetric: the Wulff point *W* lies at a large distance from the island center. Yet the island shape is perfectly symmetric. The polar free-energy plot is also very asymmetric with respect to the Wulff point. For example, the minimum on the right is much deeper than the one on the left. At first sight, the polar energy plot may look symmetric with respect to a displaced origin, like the island shape, but this is not the case. The island contour and the polar free-energy plot coincide in four points. The first two lie on the short axis of the island. The other two points do not lie on the long axis of the island, but a little distance to the left of it. These two points coincide with the highest values of the step free energy.[14]

Figure 5 demonstrates how the symmetry in the island contour arises. The center (symmetry point) of the island contour lies at a distance *d* from the Wulff point *W*. To find

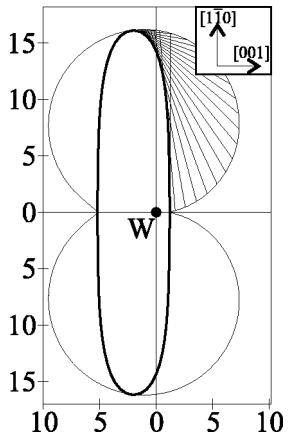

FIG. 4. The symmetric contour of a vacancy island on Au(110) (1×2) obtained via the Wulff construction of an asymmetric polar free-energy plot. The energies are expressed in meV/Å. The directions of the $[1\bar{1}0]$ and [001] steps are indicated by the arrows.

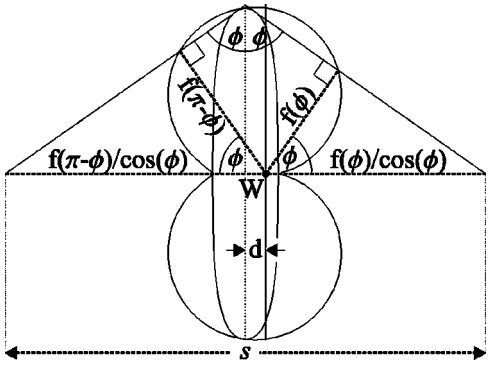

FIG. 5. Condition on the step free energy to produce a symmetric island contour via the Wulff construction. As derived in the text, when the condition $f(\pi-\phi)=f(\phi)+2d\cos(\phi)$ is satisfied for all angles ϕ, the shape of the island is mirror symmetric with respect to a symmetry axis at a distance *d* from the Wulff point *W*.

the condition for shape symmetry, we apply the inverse Wulff construction to the island shape. Let us select two points on the symmetric island contour: one arbitrary point and its mirror image with respect to the island's symmetry axis. Through these two points lines are drawn tangential to the island. Because of the required symmetry, these two lines run under the same angle ϕ with respect to the symmetry axis. Next, we draw two lines, perpendicular to the tangent lines, which both intersect the Wulff point. The indicated lengths along these perpendicular lines are proportional to the free energies $f(\phi)$ and $f(\pi\text{-}\phi)$ of steps with orientations represented by normal vectors at angles ϕ and π-ϕ with the horizontal axis. The complete polar-step free-energy plot is constructed by repeating this operation for all angles ϕ. The symmetry condition can now easily be formulated in terms of the width *s* indicated in Fig. 5. On the one hand,

$$s=\{f(\pi-\phi)+f(\phi)\}/\cos(\phi), \tag{1}$$

while, on the other hand, the symmetry requires

$$s=2\{d+f(\phi)/\cos(\phi)\}. \tag{2}$$

If we combine Eqs. (1) and (2), it follows that the Wulff construction produces a symmetric island with a distance *d* between the island center and the Wulff point, if for all angles ϕ

$$f(\pi-\phi)=f(\phi)+2d\cos(\phi). \tag{3}$$

This may seem a very peculiar condition, but as we show in the next section, it is relatively easily satisfied on Au(110) and similar surfaces.

IV. STEP FREE ENERGY

To calculate the equilibrium shape of vacancy islands on Au(110) we have to know the free energy *f* per unit length of an infinitely long step, for all step directions. In this section we derive expressions for the orientation-dependent step free energy $f(\phi)$ for a simple model of the Au(110) surface, in which the formation energy of every step configuration is a simple sum of energies of individual step segments along the

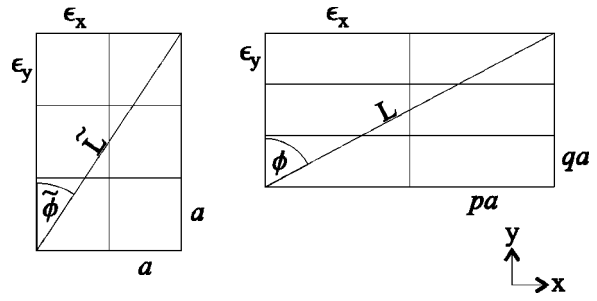

FIG. 6. Steps on a square lattice, with lattice spacing a, and on a rectangular lattice, with lattice spacings pa and qa. The steps span the same numbers of step segments, in both the x direction and the y direction. If a step segment on the square lattice in the x direction has the same energy ϵ_x as a step segment on the rectangular lattice in the x direction, and the same holds for the y direction, then the total step free energy F is equal for the two steps. The relations between the corresponding step lengths $L \leftrightarrow \tilde{L}$ and angles $\phi \leftrightarrow \tilde{\phi}$ are derived in the text.

[001] and $[1\bar{1}0]$ directions. We first describe how to obtain $f(\phi)$ for a surface with rectangular symmetry from the step free energy for square symmetry. In order to apply the result to the special case of Au(110), which has two different types of steps along $[1\bar{1}0]$, we separate f into the ground-state energy and the free-energy contribution stemming from fluctuations in the step position. Finally, we derive an explicit expression for $f(\phi)$ within the two-dimensional Ising model as well as two different approximations, each of which ignores fluctuations along one particular direction.

A. From a square lattice to a rectangular lattice

It is straightforward to derive an expression for the free energy per unit length of a step on a rectangular surface, $f_{rect}(\epsilon_x, \epsilon_y, \phi, T)$, starting from a model that describes the step free energy $f_{sq}(\epsilon_x, \epsilon_y, \phi, T)$ on a square surface, on the basis of the formation energies of individual step segments (e.g., lattice units) along the x direction, ϵ_x, and along the y direction, ϵ_y. Compare the square and rectangular geometries in Fig. 6. The step on the rectangular surface making an angle ϕ with the y axis and with a length L has the same total free energy F as the step on the square surface, with angle $\tilde{\phi}$ and length $\tilde{L}$. If the lattice spacings of the rectangular surface are pa and qa, the following relations hold:

$$\frac{\tilde{L}}{L} = \frac{\sin\phi}{p \sin\tilde{\phi}} \tag{4}$$

and

$$\tilde{\phi} = \arctan\left(\frac{q}{p}\tan(\phi)\right). \tag{5}$$

Therefore, the free energy on the rectangular surface becomes

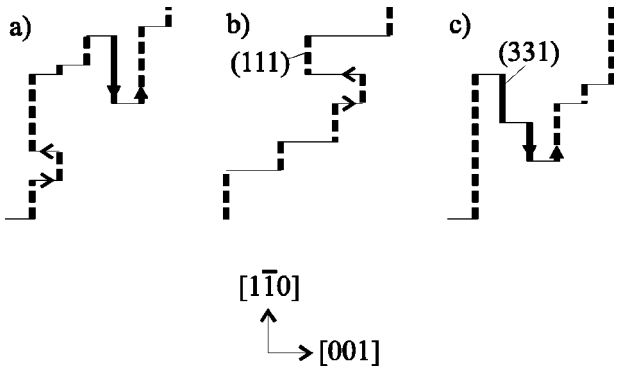

FIG. 7. Schematic representation of step configurations on Au(110). (a) A step configuration with fluctuations in both the [001] and $[1\bar{1}0]$ directions. Configurations with both types of fluctuations are considered in the two-dimensional Ising model (see Sec. IV D). (b) A step configuration with fluctuations only in the [001] direction, as considered by the perpendicular fluctuation approximation of Carlon and van Beijeren (Ref. 19) (see Sec. IV E). (c) A step with fluctuations only in the $[1\bar{1}0]$ direction, as considered in the alternative, parallel fluctuation approximation (see Sec. IV F).

$$\begin{aligned} f_{rect}(\epsilon_x, \epsilon_y, \phi, T) &= \frac{F(\epsilon_x, \epsilon_y, \phi, T)}{L} \\ &= \frac{\tilde{L}}{L} f_{sq}(\epsilon_x, \epsilon_y, \tilde{\phi}, T) \\ &= \frac{\sin(\phi)}{p \sin\left[\arctan\left(\frac{q}{p}\tan(\phi)\right)\right]} \\ &\quad \times f_{sq}\left(\epsilon_x, \epsilon_y, \arctan\left(\frac{q}{p}\tan(\phi)\right), T\right). \end{aligned} \tag{6}$$

B. Energetics of a missing-row surface

Figure 7(a) is a schematic representation of a piece of step on Au(110). It is built up from three types of unit elements: (i) a single step segment along the [001] direction, with a length of the MRR period, i.e., 2 times the lattice constant of Au of $a = 4.08$ Å, and a formation energy $\epsilon_{[001]}$; (ii) a single segment of a step along the $[1\bar{1}0]$ direction of the (111) type, with a length of the atomic spacing along this direction, of $a/\sqrt{2}$, and an energy ϵ_{111}; (iii) a single (331)-step segment, also with a length of $a/\sqrt{2}$, but with an energy ϵ_{331}. The combination of a single (331)-step segment and a single (111)-step segment forms the lowest-energy excitation of a [001] step. We will refer to such fluctuations as parallel fluctuations (bold arrows in Fig. 7), because the extra step segments are parallel to the missing rows. Similarly, we define the combination of two [001]-step segments in opposite directions as a perpendicular fluctuation (thin arrows in Fig. 7). From Ref. 9 we know that the energies of (111) and (331) kinks are equal to within 6 permille and that they are, to a very good approximation, equal to the energy of a [001]-step segment[15] (see Sec. III). With this information, we can ex-

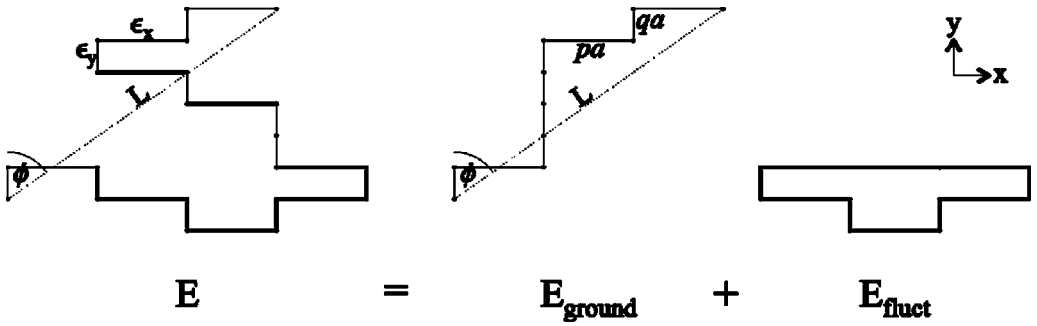

FIG. 8. A step configuration with length L and angle ϕ on a rectangular lattice with lattice spacings pa in the x direction and qa in the y direction and step segment energies ϵ_x and ϵ_y. The total energy E of the step configuration can be split into a ground-state contribution E_{ground} and a fluctuation contribution E_{fluct}. The step segments that contribute to the ground-state energy (thin lines) can be seen by looking from the left and from the top to the step configuration. The remaining step segments, which form the fluctuations, can be put into a closed loop, as there are as many step segments upwards as downwards and as many to the left as to the right.

press the formation energy of any step configuration as the sum of step segment formation energies of the three types, introduced above.

C. Separating energy contributions from the ground state and from fluctuations

We face a problem when trying to derive the free energy of a step on a missing-row reconstructed surface f_{MRR}, starting from a model for the step free energy $f_{rect}(\epsilon_x,\epsilon_y,\phi,T)$ on an unreconstructed, rectangular surface. While on the unreconstructed surface there is just one type of step segment parallel to the MR's, on the reconstructed surface there exist two. The solution to this problem is not difficult, but has, to our knowledge, not been presented before. Our method is to distinguish between two separate contributions to the free energy of a step on the simple rectangular lattice (see Fig. 8): namely, the ground-state energy and free energy due to fluctuations in the step position. Any configuration of a finite piece of step, which spans a distance L along direction ϕ, consists of at least $L|\sin\phi|/pa$ x-step segments and $L|\cos\phi|/qa$ y-step segments, where pa and qa are the lengths of step segments along x and y. Therefore, the ground-state contribution to the step free energy per unit length is

$$e_{ground}=\frac{E_{ground}}{L}=\frac{\epsilon_x}{pa}|\sin\phi|+\frac{\epsilon_y}{qa}|\cos\phi|. \tag{7}$$

If the ground-state energy is subtracted from f_{rect}, the remaining part of the free energy is due to fluctuations:

$$f_{fluct}=f_{rect}-e_{ground}=f_{rect}-\frac{\epsilon_x}{pa}|\sin\phi|-\frac{\epsilon_y}{qa}|\cos\phi|. \tag{8}$$

One part of the fluctuation free energy f_{fluct} accounts for the configurational entropy of the step segments of which the formation energy is already covered by e_{ground}. In addition, f_{fluct} contains the free energy related to the introduction of extra step segments, i.e., of parallel and perpendicular fluctuations in the step configuration, as introduced in Sec. IV B. In these fluctuations, the step segments always come in pairs, i.e., (111)+(331) or $2\times[001]$. We can now rewrite Eqs. (7) and (8) to describe the specific case of a missing-row reconstructed surface. We choose $\phi=0$ for a (111) step and consequently $\phi=\pi$ for a (331) step. For $-\pi/2\leqslant\phi\leqslant\pi/2$, the ground state of a configuration consists of only (111)-step segments and [001]-step segments. For these angles, we associate ϵ_x with $\epsilon_{[001]}$ and ϵ_y with ϵ_{111} in the ground-state contribution [Eq. (7)]. For $\pi/2\leqslant\phi\leqslant3\pi/2$ the ground-state configuration consists of only (331)-step segments and [001]-step segments, so that we substitute ϵ_y with ϵ_{331}, while ϵ_x still stands for $\epsilon_{[001]}$ in Eq. (7). Because a fluctuation in the y direction is a combination of one (111) and one (331) step, ϵ_y has to be replaced with $(\epsilon_{111}+\epsilon_{331})/2$ in the fluctuation term [Eq. (8)], while also, for this term, $\epsilon_x=\epsilon_{[001]}$. With $p=2$ and $q=1/\sqrt{2}$, we find for the step free energy on a missing-row reconstructed surface:

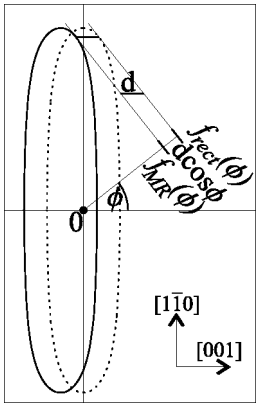

FIG. 9. If the step free energies of two different Wulff constructions differ by an amount $d\cos\phi$ where ϕ is the angle of the step with the $[1\bar{1}0]$ direction, the two resulting island shapes are identical. If the two Wulff constructions are plotted in one polar diagram, the two islands are shifted with respect to each other over a distance d in the [001] direction. This is the case for an island on a MRR surface with step segment energies ϵ_{111} and ϵ_{331} in the $[1\bar{1}0]$ direction (solid curve) and an island on a simple rectangular surface with a step segment energy $(\epsilon_{111}+\epsilon_{331})/2$ in the $[1\bar{1}0]$ direction (dotted curve).

$$
\begin{aligned}
&f_{MR}(\epsilon_{111},\epsilon_{331},\epsilon_{[001]},\phi,T)\\
&=f_{fluct}\left(\frac{\epsilon_{111}+\epsilon_{331}}{2},\epsilon_{[001]},\phi,T\right)+\begin{cases} e_{ground}(\epsilon_{111},\epsilon_{[001]},\phi), & \phi\in\left[-\frac{\pi}{2},\frac{\pi}{2}\right]\\ e_{ground}(\epsilon_{331},\epsilon_{[001]},\phi), & \phi\in\left[\frac{\pi}{2},\frac{3\pi}{2}\right]\end{cases}\\
&=\underbrace{\frac{\epsilon_{[001]}}{2a}|\sin\phi|+\frac{\epsilon_{111}-\epsilon_{331}}{\sqrt{2}a}\cos\phi+\frac{\epsilon_{111}+\epsilon_{331}}{\sqrt{2}a}|\cos\phi|}_{e_{ground}}\\
&\quad\underbrace{+f_{rect}\left(\frac{\epsilon_{111}+\epsilon_{331}}{2},\epsilon_{[001]},\phi,T\right)-\frac{\epsilon_{[001]}}{2a}|\sin\phi|-\frac{\epsilon_{111}+\epsilon_{331}}{\sqrt{2}a}|\cos\phi|}_{f_{fluct}}\\
&=\frac{\epsilon_{111}-\epsilon_{331}}{\sqrt{2}a}\cos\phi+f_{rect}\left(\frac{\epsilon_{111}+\epsilon_{331}}{2},\epsilon_{[001]},\phi,T\right).
\end{aligned}
\tag{9}
$$

It follows from Eq. (9) in combination with Eq. (3) that the Wulff construction on our model MRR surface produces a symmetric island shape with a distance $d=(\epsilon_{331}-\epsilon_{111})/\sqrt{2}a$ between the island center and the Wulff point, irrespective of the specific model employed for f_{rect}.

According to Eq. (9), the difference between the step free energies f_{MR} for a MRR surface and f_{rect} for a simple rectangular surface is equal to $d\cos\phi$, for each step orientation ϕ (see Fig. 9). The corresponding displacement of $d\cos\phi$ between the tangent lines in the two Wulff constructions is equivalent to a horizontal, i.e., [001]-oriented shift over a distance d for all orientations ϕ. As a result, the entire Wulff shape is translated along [001] and is completely identical to the shape for a surface with equal energies for the two step types along $[1\bar{1}0]$, of $(\epsilon_{111}+\epsilon_{331})/2$. This has to be so, because a substitution of $(\epsilon_{111}+\epsilon_{331})/2$ for ϵ_{111} as well as for ϵ_{331} leaves the creation energy of an island with an arbitrary contour shape unchanged. Note that the polar free-energy plots *do* have different shapes for the two cases.

In the following three subsections we will apply Eq. (9) to three different choices for f_{rect}. The first model that we will treat is the two-dimensional anisotropic Ising model,[16,17] which considers both parallel and perpendicular fluctuations and gives the exact step free energy for all temperatures and angles, as long as the energy can be calculated as a simple sum of step segment energies. The two-dimensional Ising model also takes into consideration step configurations with clusters of adatoms on the lower terrace and vacancy clusters inside the higher terrace. The second and third choices for f_{rect} are for two different applications of the anisotropic one-dimensional solid-on-solid model,[18] which allows only fluctuations in a single direction. First we will study the case that only fluctuations perpendicular to the missing row direction are allowed, and then we will consider the one-dimensional solid-on-solid model with only fluctuations parallel to the MR's. In both one-dimensional solid-on-solid models, configurations with adatom or vacancy clusters are forbidden. Results for the three models will be compared in Sec. V.

D. Two-dimensional Ising model

First, we calculate the step free energy on Au(110) using the two-dimensional anisotropic Ising model, in which both parallel and perpendicular fluctuations are allowed. Equation (3) of Ref. 17, in combination with Eqs. (6) and (9), leads to the step free energy

$$
\begin{aligned}
f_{Ising}(\phi)=&\frac{1}{2\beta a}\alpha_1\left[\arctan\left(\frac{\tan\phi}{\sqrt{8}}\right)\right]|\sin\phi|\\
&+\frac{\sqrt{2}}{\beta a}\alpha_2\left[\arctan\left(\frac{\tan\phi}{\sqrt{8}}\right)\right]|\cos\phi|\\
&+\frac{\epsilon_{111}-\epsilon_{331}}{\sqrt{2}a}\cos\phi,
\end{aligned}
\tag{10}
$$

with

$$
\alpha_1(\phi)=\operatorname{arccosh}\left[\frac{(c^2-n^2)\sin^2\phi+m^2\cos^2\phi}{mc(\sin^2\phi)+jm}\right], \tag{11}
$$

$$
\alpha_2(\phi)=\operatorname{arccosh}\left[\frac{(c^2-m^2)\cos^2\phi+n^2\sin^2\phi}{nc(\cos^2\phi)+jn}\right], \tag{12}
$$

$$
j=\sqrt{\left(\frac{c}{2}\sin 2\phi\right)^2+\cos 2\phi(m^2\cos^2\phi-n^2\sin^2\phi)}, \tag{13}
$$

$$
c=(1+e^{-2\beta\epsilon_{[001]}})(1+e^{-\beta(\epsilon_{111}+\epsilon_{331})}), \tag{14}
$$

$$m = 2e^{-\beta\epsilon_{[001]}}(1-e^{-\beta(\epsilon_{111}+\epsilon_{331})}), \tag{15}$$

and

$$n = 2e^{-\beta(\epsilon_{111}+\epsilon_{331})/2}(1-e^{-2\beta\epsilon_{[001]}}). \tag{16}$$

The factors $\sqrt{2}$ for the cosine, 1/2 for the sine, and $1/\sqrt{8}$ for the tangent reflect the ratio between the lengths of step segments parallel and perpendicular to the missing rows.

E. Perpendicular fluctuation approximation

Next, we calculate the step free energy on Au(110) using a one-dimensional solid-on-solid model.[18] This model considers steps containing excursions in only one direction. Because we know that a (331)-step segment is higher in energy than a (111)-step segment, it seems logical to consider only step configurations consisting of (111)- and [001]-step segments, such as shown in Fig. 7(b). This approximation was used by Carlon and van Beijeren[19] for the calculation of the free energy of (111) steps, probably because it avoided the difficulty introduced by the existence of two different step types along the $[1\bar{1}0]$ direction. We will call this model the perpendicular fluctuation approximation, because the allowed fluctuations are all in the direction perpendicular to the missing rows. For steps parallel to the missing rows ($\phi \approx 0$ and $\phi \approx \pi$) this is a good approximation, but for steps perpendicular to the missing rows ($\phi \approx \pi/2$ and $\phi \approx 3\pi/2$) the model breaks down, because such steps simply cannot fluctuate in the [001] direction. In this model, the expression for the free energy per unit length of an infinitely long (111) step with an angle ϕ to the missing rows has been shown to be[18,19]

$$\begin{aligned} f_{\perp,111}(\phi) = {} & \epsilon_{[001]}\frac{|\sin\phi|}{2a} + \epsilon_{111}\frac{\sqrt{2}|\cos\phi|}{a} \\ & + [\ln\overline{z}(\phi) - \beta\epsilon_{[001]}]\frac{|\sin\phi|}{2\beta a} \\ & + \left[\ln\left(\frac{2\cosh(\beta\epsilon_{[001]}) - [\overline{z}(\phi) + 1/\overline{z}(\phi)]}{2\sinh(\beta\epsilon_{[001]})}\right)\right] \\ & \times \frac{\sqrt{2}|\cos\phi|}{\beta a}, \end{aligned} \tag{17}$$

where $\beta = 1/(kT)$ and

$$\overline{z}(\phi) = \frac{\cosh(\beta\epsilon_{[001]})\overline{t}(\phi) + \sqrt{1+\sinh^2(\beta\epsilon_{[001]})\overline{t}^2(\phi)}}{1+\overline{t}(\phi)}, \tag{18}$$

with

$$\overline{t}(\phi) = |\tan(\phi)|/2\sqrt{2}, \tag{19}$$

and a is the lattice constant of Au (4.08 Å). The first two terms in Eq. (17) represent the ground-state energy of the step. By substitution of Eq. (17) into Eq. (9), the expression for the step free energy in the perpendicular fluctuation approximation becomes

$$\begin{aligned} f_{\perp}(\phi) = {} & [\ln\overline{z}(\phi)]\frac{|\sin\phi|}{2\beta a} + \frac{\epsilon_{111}-\epsilon_{331}}{\sqrt{2}a}\cos(\phi) \\ & + \left[\beta\frac{\epsilon_{111}+\epsilon_{331}}{2} \right. \\ & \left. + \ln\left(\frac{2\cosh(\beta\epsilon_{[001]}) - [\overline{z}(\phi) + 1/\overline{z}(\phi)]}{2\sinh(\beta\epsilon_{[001]})}\right)\right] \\ & \times \frac{\sqrt{2}|\cos\phi|}{\beta a}. \end{aligned} \tag{20}$$

F. Parallel fluctuation approximation

By contrast with the assumption underlying the perpendicular fluctuation approximation, perpendicular fluctuations are never observed in STM images (at low and modest temperatures), and they are only expected to occur at high temperatures near the phase transition of the Au(110) surface. At lower temperatures, almost all fluctuations are parallel to the missing-row (MR) direction,[20–22] as illustrated in Fig. 7(c). The reason for this is that the formation energy of a [001]-step segment, perpendicular to the MR's, is high, $\epsilon_{[001]} = 200$ meV.[11] The formation energy of a single perpendicular fluctuation is 2 times this amount, 400 meV. The formation energy of a parallel fluctuation is the sum of the formation energies ϵ_{331} of a (331)-step segment and ϵ_{111} of a (111)-step segment, which is as low as 19 meV.[11,23] Therefore a model that considers only steps with parallel fluctuations should provide a much better approximation to the step free energy. We will call this the parallel fluctuation approximation. It is good for steps perpendicular to the MR's ($\phi \approx \pi/2$ and $\phi \approx 3\pi/2$), but it makes less sense for steps parallel to the MR's ($\phi \approx 0$ and $\phi \approx \pi$), because the latter steps can only contain perpendicular fluctuations.

The solid-on-solid model [e.g., Eq. (7) of Ref. 17], in combination with Eqs. (6) and (9), immediately produces the step free energy per unit length in the parallel fluctuation approximation:

$$\begin{aligned} f_{\parallel}(\phi) = {} & \frac{\epsilon_{111}-\epsilon_{331}}{\sqrt{2}a}\cos\phi + \frac{\ln z(\phi)\sqrt{2}|\cos\phi|}{\beta a} + \epsilon_{[001]}\frac{|\sin\phi|}{2a} \\ & + \ln\left(\frac{2\cosh(\beta(\epsilon_{331}+\epsilon_{111})/2) - [z(\phi)+1/z(\phi)]}{2\sinh(\beta(\epsilon_{331}+\epsilon_{111})/2)}\right) \\ & \times \frac{|\sin\phi|}{2\beta a}, \end{aligned} \tag{21}$$

with

$$z(\phi)=\frac{\cosh[\beta(\epsilon_{331}+\epsilon_{111})/2]t(\phi)+\sqrt{1+\sinh^2[\beta(\epsilon_{331}+\epsilon_{111})/2]t^2(\phi)}}{1+t(\phi)} \tag{22}$$

and

$$t(\phi)=2\sqrt{2}|\cot(\phi)|. \tag{23}$$

This result can also be obtained from Eq. (17) by an appropriate scale transformation and replacement of step segment energies for the ground state of the step and for the fluctuations.

V. EQUILIBRIUM ISLAND SHAPE

In this section we employ the three descriptions of the step free energy $f(\phi)$ on Au(110) to predict the equilibrium shapes of two different types of islands on this surface, namely, the asymmetric islands, introduced in Secs. II and III, and a symmetric-type island that can be formed by more complex step combinations.

A. Free energy of asymmetric islands

The temperature-dependent contour of the asymmetric vacancy islands can be seen in Fig. 10, for each of the three approximations to the step free-energy. The thin lines are the free energy curves and the thick lines are the island contours. The dotted lines represent the Ising model and the parallel fluctuation approximation, which cannot be distinguished on this scale for temperatures up to at least 400 K. At 600 K, the Ising free energy and island contour are described better by the results from the perpendicular fluctuation approximation, for a narrow range of step orientations around $[1\bar{1}0]$ indicated with the solid lines. On this scale, the inner contours of the parallel and perpendicular fluctuation free-energy curves coincide for all temperatures with the corresponding curve of the Ising model, and the same holds for the island shapes. In reality, both solid-on-solid-approximations coincide with the exact Ising expression for the step free energy only at 0 K, as there is no entropy in play. However, because both approximations do not consider *all* possible step configurations (Fig. 7), they both overestimate all free-energy values at all nonzero temperatures. This means, that for each (ϕ,T) combination, the *lowest* step free energy predicted by the two approximations is closest to the *true* step free energy of the Ising model.

The previous argument is not entirely correct, because there is, apart from the allowed directions of fluctuations, one additional difference between the Ising model and the solid-on-solid models: the Ising model includes the possibility of forming extra clusters of adatoms on the lower terrace and clusters of vacancies inside the higher terrace, which is not permitted in the solid-on-solid models. The step free energy is defined as the difference between the free energies of a surface with and without a step. When a step is introduced, the contribution to the free energy of the adatom and vacancy clusters is lowered, since the clusters at the position of the step are forbidden. This increases the Ising step free energy slightly. The surprising consequence is that the results for the

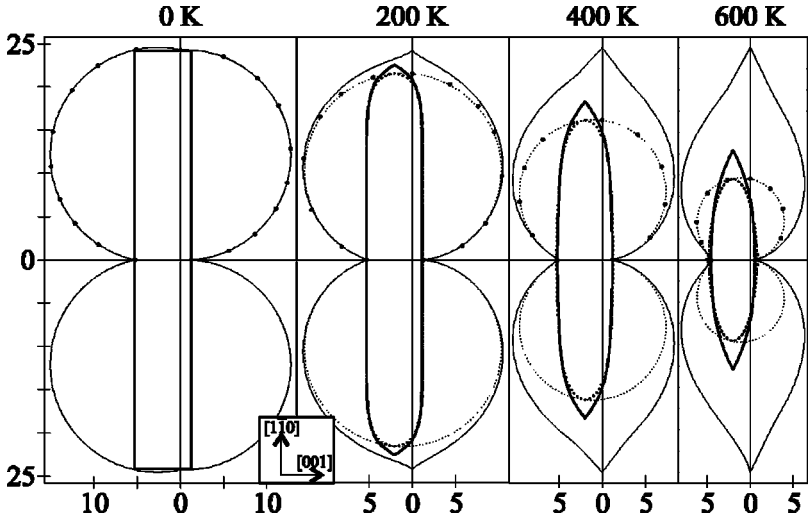

FIG. 10. Wulff constructions for the Ising model and the parallel fluctuation approximation (dotted curves) and the perpendicular fluctuation approximation (solid curves), for different temperatures. The thin curves are the step free-energies and the thick curves are the equilibrium island shapes. On this scale, the step free energy of the Ising model coincides with the combined inner contour of the free energy curves for the two solid-on-solid approximations. Similarly, the Ising island shape follows the inner contour of the two other island shapes. For all three models the shape is perfectly symmetric at all temperatures. The dots are the results of Monte Carlo calculations of the step free energy. The energies are indicated as meV/Å. Used step segment energies are $\epsilon_{111}=3.7$ meV, $\epsilon_{331}=15.3$ meV, and $\epsilon_{[001]}=200$ meV (Refs. 11 and 15). The directions of the $[1\bar{1}0]$ and [001] steps are indicated by the arrows.

parallel fluctuation approximation are identical to those for the Ising model for the [001] step orientation, while the results for the perpendicular approximation are identical to those for the Ising model for both types of $[1\bar{1}0]$-steps. These identities hold for all temperatures.[24] However, for all other directions, the free energy of the Ising model is lower than the free energies of both solid-on-solid approximations.[25]

Parallel fluctuations exist already at low temperatures, due to their low creation energy. Therefore, the free energy of a [001] step, which can, to first approximation (no ''overhangs,'' i.e., no perpendicular fluctuations on top of parallel excursions), only contain parallel fluctuations, is approximated best by the parallel fluctuation model, rather than by the perpendicular fluctuation model, which just gives the creation energy for this step direction. Because perpendicular fluctuations occur only at high temperatures, due to their high creation energy, the free energy of a $[1\bar{1}0]$ step, which can, to first approximation, only contain perpendicular fluctuations, is almost equal to its creation energy and can therefore be described by either of the two solid-on-solid models for temperatures that are not too high. When perpendicular fluctuations become important, the parallel fluctuation approximation fails for the $[1\bar{1}0]$ steps. However, this is the case only at very high temperatures. As can be seen from Fig. 10, $f_{\parallel}$ is indeed the better description of the step free energy for most step directions at all temperatures. Only for steps almost parallel to the $[1\bar{1}0]$ direction, $f_{\perp}$ yields a better approximation. As a consequence, the island shape predicted by the perpendicular approximation lies outside the one predicted by the parallel approximation, except for small portions on the $[1\bar{1}0]$ sides of the shape that lie on the inside. When the temperature is raised, these portions increase. This can be seen from the shapes at 600 K in Fig. 10. The figure also shows results of Monte Carlo (MC) calculations of the free energy (see the Appendix). In the MC simulation, both parallel and perpendicular fluctuations were allowed. The difference between the model used for the MC calculations and the Ising model is that the MC simulation did not allow for step configurations with adatom clusters on the lower terrace or vacancies in the higher terrace. Nevertheless, even for high temperatures, the MC results coincide nicely with the free energy from the Ising model, which shows that such clusters have a negligible effect on the step free energies.

B. Temperature dependence of asymmetric islands

The contour shapes of the islands in Fig. 10 are, for all temperatures, totally symmetric with respect to the same symmetry axis at a distance $d=(\epsilon_{331}-\epsilon_{111})/\sqrt{2}$ from the Wulff point. At 0 K the island shape is rectangular. For any nonzero temperature, there are no straight steps, steps being rough at all finite temperatures. When the temperature is increased, the contour shape initially becomes shorter, while the width stays (nearly) constant. At 600 K, also a change in the width can be seen. When the temperature is increased even further, the step free energy of the (111) step becomes zero. At that temperature, the surface can create (111) steps without raising its free energy. As a consequence, the surface goes through the so-called roughening transition, which is of the Kosterlitz-Thouless type.[26] It may seem that a proliferation of (111) steps is impossible without the generation of an equally high density of (331) steps. This would mean that the islands, including (111) steps with a negative free energy, would be (meta)stable, because the sum of the (111)- and (331)-step free energies is positive. However, alternative step configurations are possible, which have only (111) steps, and completely avoid (331) steps.[11] Therefore, a Wulff construction with a Wulff point lying outside the equilibrium island shape, such as proposed by van Beijeren and Nolden,[12] will not occur on this surface. In reality, another phase transition is thought to take place close to, but possibly below the roughening transition. When the free energy of domain boundaries in the MRR becomes zero, the MRR vanishes. This is called the deconstruction transition, first found by Wolf *et al.* in a low-energy electron diffraction (LEED) experiment on Au(110).[27] Bak predicted that the deconstruction is of the Ising type,[28] after which Campuzano *et al.* were the first to report experimental evidence for the Ising character of the transition.[29] The first detailed theoretical description of the transition for the specific case of a MR reconstructed surface, such as Au(110), was given by Villain and Vilfan.[30] The interplay between the two phase transitions, noticed already in Ref. 30, was worked out by Vilfan and Villain[31] and den Nijs.[32] Sprösser *et al.* found the two transitions to occur on Au(110) at separate temperatures in a thermal energy atom scattering (TEAS) experiment.[33] A similar conclusion was reached in medium-energy ion scattering (MEIS) experiments by Romahn *et al.*[34] Mazzeo *et al.*[35] and Barbier *et al.*[36] also found separate transitions in Monte Carlo simulation studies. Sturmat *et al.* have attempted to observe the two transitions with STM.[20,21]

If the deconstruction transition takes place at a lower temperature, separate from the roughening transition, the roughening transition takes place on a deconstructed surface, the so-called disordered flat phase.[37] The models, treated in the present paper, are only valid for the (1×2) reconstructed Au(110) surface, i.e., not for the disordered flat phase. They should therefore be expected to yield bad estimates for the roughening temperature.

C. Symmetric islands

The symmetric shape with both (111) and (331) steps, described in the previous section and illustrated in Figs. 4 and 10, is only observed for relatively small vacancy islands (typically below 80 nm^2). All structures on Au(110) with (331) steps appear to be metastable.[9] Although (331)-step segments occur in combination with (111)-step segments as fluctuations in [001] steps, extended (331) steps are only found in experiments, when created artificially by low dose sputtering of the Au(110) surface. All larger adatom and vacancy islands adopt alternative configurations, with (111) steps on both sides. The resulting problem with the phase of the missing-row reconstruction (see Fig. 2) is eliminated by introducing networks of steps.[11] A pattern of crossing steps is

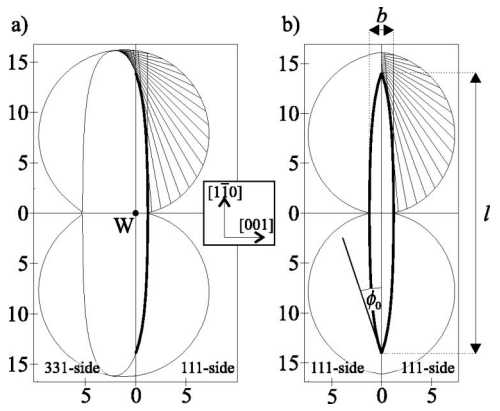

FIG. 11. (a) Wulff construction of a metastable vacancy island in Au(110) for $T=400$ K, according to the Ising model. The stable equilibrium shape of islands on Au(110), with only (111)-type steps, can be obtained by mirroring the (111) side (thick line) of the asymmetric Wulff construction in the (vertical) $[1\bar{1}0]$ axis through the Wulff point. (b) Wulff construction of the stable equilibrium shape of adatom and vacancy islands for $T=400$ K. The aspect ratio is defined as l/b and $2\phi_0$ is the sharp angle of the almond-shaped island. The energies are expressed in meV/Å. The directions of the $[1\bar{1}0]$ and [001] steps are indicated by the arrows.

formed with one family of curved steps forming the right-hand sides of islands and a mirrored family of intersecting steps forming the left-hand sides. In this way, all steps are of the low-energy (111) type, while the creation of domain boundaries in the MRR is avoided. A second solution exists in configurations with four steps, two upward and two downward, which all end in the same two points, which are called termination sites.[11] This results in, e.g., double-height islands, where the upper and lower levels ''touch'' in two points.[11]

The contour shape of vacancy and adatom islands on Au(110) with (111) steps on both sides can easily be derived from Eq. (10), (20), or (21) via a slightly modified Wulff construction. The polar-step free-energy plot is made symmetric in this case, by forcing it to consist of the free energy of (111)-like steps on both sides. Therefore, we can find the shape by mirroring the right part of the step free energy plot and island shape of Fig. 11(a) in the vertical $[1\bar{1}0]$ axis through the Wulff point [Fig. 11(b)]. The formulas for the step free energy of the almonds in the Ising model and in the perpendicular and parallel fluctuation approximations can therefore easily be obtained from the asymmetric island free energies, Eqs. (10), (20), and (21), by replacing all $\cos\phi$ terms with $|\cos\phi|$. The result has a peculiar, sharp-cornered, almondlike shape, which was also predicted in Ref. 19 from the Wulff construction within the perpendicular fluctuation approximation [Eq. (20)] and which is indeed observed on Au(110).[11] In Ref. 15, the energies of the different step segments, ϵ_{331}, ϵ_{111}, and $\epsilon_{[001]}$, have been determined from fits of the Wulff construction in Fig. 11(b) to the observed shapes at a range of temperatures. In particular, the angle $2\phi_0(\epsilon_{331},\epsilon_{111},\epsilon_{[001]},T)$ of the sharp corner of the observed almonds [Fig. 11(b)] and the island aspect ratio $A(\epsilon_{331},\epsilon_{111},\epsilon_{[001]},T)=l/b$, with l the length and b the width

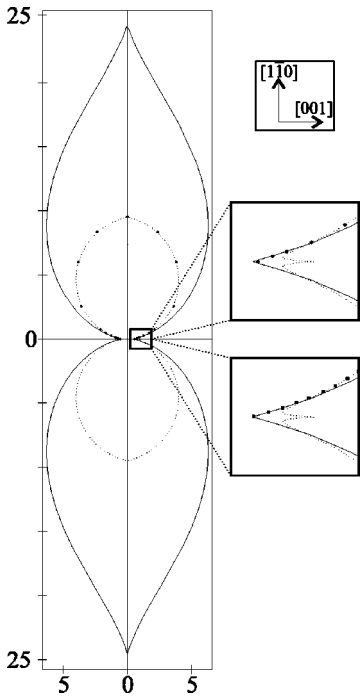

FIG. 12. Comparison of f_{Ising}, $f_\perp$, $f_\parallel$ and MC calculations for almond-shaped islands at $T=600$ K. The energies are expressed in meV/Å. The directions of the $[1\bar{1}0]$ and [001] steps are indicated by the arrows. On the scale of the left panel, f_{Ising} and $f_\parallel$ (dotted line) coincide, while $f_\perp$ (solid) is higher for almost all angles. As can be seen from the magnified insets, only for a small range of orientations around the $[1\bar{1}0]$-step direction is $f_\perp$ lower than $f_\parallel$. In the lower magnified inset, free-energy values obtained with the Ising model are indicated with square dots. On this scale, the free-energy values obtained with the Ising model cannot be distinguished from the inner contour of the free energies of the two solid-on-solid models. $f_\perp$ has a minimum for steps along $[1\bar{1}0]$ and a maximum cusp for steps along [001], while $f_\parallel$ has maxima (cusps) in both directions. The dots are the results of Monte Carlo simulations of the free energy. In the upper magnified inset it can be seen that the Monte Carlo points always almost coincide with the Ising model and the lower of the two solid-on-solid free energy values. The fact that most of the values obtained from the MC simulation are slightly higher is a consequence of the finite length of the steps in the simulation.

of the contour shape [Fig. 11(b)], were fitted. It was possible to obtain values for all step free energies, because the sum $\epsilon_{331}+\epsilon_{111}=19\pm1$ meV had been measured independently in Ref. 23. The results for the step segment energies are $\epsilon_{111}=3.7\pm0.5$ meV, $\epsilon_{331}=15.3\pm1.1$ meV, and $\epsilon_{[001]}=200\pm60$ meV. These are the values used for all Wulff constructions in this paper.

Figure 12 compares f_{Ising}, $f_\parallel$, $f_\perp$, and Monte Carlo simulation results for almond-shaped islands at $T=600$ K. As for the asymmetric islands in Sec. V A, the exact Ising shape is approximated best by $f_\parallel$ over almost the entire range of step orientations. There is only a small range around the $[1\bar{1}0]$-step direction, for which $f_\perp$ provides the better approximation to f_{Ising}. It is exactly this range that determines the width b of the almond [see Fig. 11(b)] via the Wulff

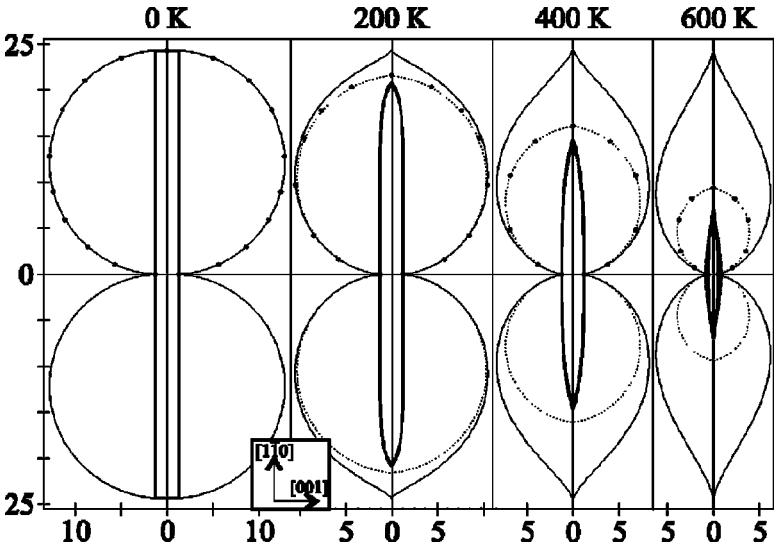

FIG. 13. Polar free-energy plots for the Ising model and the parallel fluctuation approximation (dotted curves), the perpendicular fluctuation approximation (solid curves), and from MC calculations (dots), of (111)-like steps on Au(110) for different temperatures, together with the equilibrium almond island shapes (thick curves). As the temperature rises, the aspect ratio initially decreases, then increases again, and finally diverges when $f(\phi=0)$ decreases to zero. The energies are expressed in meV/Å. The directions of the $[1\bar{1}0]$ and [001] steps are indicated by the arrows.

construction. It is less straightforward to see which portion of the free-energy plot determines the length l of the almond. Via the Wulff construction, the end points of the almond shape correspond to the value of the free energy at the almond angle ϕ_0 [see Fig. 11(b)]. For temperatures below 625 K, when ϕ_0 is at least a few degrees, $f_{\parallel}(\phi_0)$ is smaller than $f_{\perp}(\phi_0)$, and the length l, obtained from the Ising model, is described most accurately by $f_{\parallel}$. For very high temperatures (>625 K), however, when the island width decreases drastically, the angle ϕ_0 also decreases and $f_{\perp}$, which is smaller than $f_{\parallel}$ for small angles, describes the length of the islands most accurately. The temperature dependence of the almond shapes will be treated further in Sec. V E.

D. Cusps in the free-energy plots: Sharp corners in the equilibrium shape

Under normal circumstances, a polar-step free-energy plot cannot contain cusps for $T>0$.[38–41] However, in Fig. 12 there are several cusps. For the $[1\bar{1}0]$-step direction, $f_{\perp}$ shows the typical minimum (no cusp) for a step in a low-index direction. By contrast, $f_{\parallel}$ has a cusp-type maximum in this direction. The reason for this is that in the parallel fluctuation model the $[1\bar{1}0]$ step cannot make any fluctuations. Therefore $f_{\parallel}(\phi=0)$ is not a function of temperature, and it is identical to the formation energy $\sqrt{2}\epsilon_{111}/a$. For the same reason $f_{\perp}$ has a cusp-type maximum for the [001] step direction, at a temperature-independent value of $\epsilon_{[001]}/2a$. Also $f_{\parallel}$ has a cusp-type maximum for the [001]-step direction, but unlike the previous cusps, this maximum is a function of temperature. At first sight this may seem impossible, because [001] steps *can* fluctuate in this model. The reason why there *is* a cusp-type maximum is that the almond-shaped island is not bounded by a single closed step, like the usual island, but rather by two different (111) steps. The cusplike maxima for the [001]-step direction of the polar-step free-energy plot are the points where the free-energy curves for the two (111) steps meet. The free energy of the Ising model shows exactly the same shape as the parallel fluctuation model around this cusp.

In general, at nonzero temperatures, equilibrium island shapes are continuously differentiable. For example, the symmetric islands on Au(110) of Fig. 10 are rectangular only at 0 K, but as soon as entropy comes into play, the corners become rounded. However, the equilibrium shape of Fig. 11(b) *does* have sharp corners. This is a peculiar consequence of the presence of a domain boundary in the surrounding terrace, at each of those points. On both sides of the domain boundary the steps can assume their most favorable orientation, independent of each other. When we compare steps at angles $+\phi$ and $-\phi$ to the [001] direction, the step with more (111)- than (331)-step segments has a lower (free) energy than the other one with more (331)- than (111)-step segments. Therefore, at any nonzero temperature, the steps on *both* sides of the domain boundary will adopt an angle at which they have more (111)- than (331)-step segments on average. As a result, the steps will meet each other under a nonzero angle at the domain boundary.

E. Temperature dependence of the symmetric Wulff construction

The temperature dependence of the almond shape can be seen in Fig. 13, together with the three models for the free energy. Thin lines are the free-energy curves and thick lines the island contours. The dotted lines represent the Ising model and the parallel fluctuation approximation, and the solid lines correspond to the perpendicular fluctuation approximation. As in Fig. 10, the inner contour of the curves for the parallel and perpendicular fluctuation approximations coincides with the Ising model on this scale. At zero temperature, the three models coincide, and the island shape is rectangular. Because the formation energy of perpendicular fluctuations is very high, the free energy of steps in the $[1\bar{1}0]$ direction hardly changes when the temperature is raised. The parallel fluctuations, however, set in at a much lower temperature, and therefore f_{Ising} and $f_{\parallel}$ immediately begin to decrease for all nonzero ϕ. As a consequence, the rectangle immediately changes into an almond and then becomes progressively shorter. As a result, the aspect ratio de-

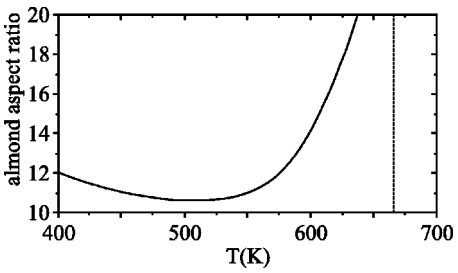

FIG. 14. Aspect ratio vs temperature for the almond shapes on Au(110). The aspect ratio first decreases and then goes to infinity at the roughening transition.

creases somewhat. Above 500 K, the effect of [001] fluctuations becomes noticeable, and the width of the almonds decreases. The aspect ratio diverges when f_{Ising} (and $f_{\perp}$) becomes zero, for steps in the $[1\bar{1}0]$ direction. This behavior of the aspect ratio is different from that of islands on a simple rectangular surface, where the step free energies in all directions vanish simultaneously. Usually, when the step free energy vanishes for one of the main directions, the step free energy for the other main direction also has to vanish, because its step fluctuations, which consist of excursions along the first main direction, involve no additional free energy. On the MRR surface, first the (111)-step free energy vanishes. The [001]-step free energy remains positive, because fluctuations in a [001] step consist of equal lengths in (111) and (331) steps. The free energy of the [001] step vanishes only when these fluctuations cost zero free energy, that is, when the free energy of a (111) step is equal to minus the free energy of a (331) step. The divergence of the aspect ratio, at the temperature at which the (111)-step free energy vanishes, corresponds to a roughening transition of the [110] surface. Figure 14 is a graph of the aspect ratio as a function of temperature, obtained from the Ising model. The vertical line is the asymptote at the roughening transition. Because the model does not consider the deconstruction transition, these results cannot be trusted at temperatures close to and above the deconstruction temperature T_d, which is believed to lie between 654 K and 765 K.[29,33,34,42,43] For the same reason, the value of the roughening temperature of $T_R = 673$ K, obtained here from the Ising model, should only be considered as a coarse estimate of the true roughening temperature of Au(110), which is thought to be about 50 K above the deconstruction temperature.[34]

VI. SUMMARY

In summary, we have considered the theory of equilibrium shapes for two types of (vacancy) islands on the (1×2) missing-row reconstructed Au(110) surface. The first type, which is metastable, can only be created artificially. It has an asymmetric internal structure, with a (331)-type step on one side and a (111)-type step on the other. Although the Wulff point does not coincide with the center of the island, the island shape observed in experiments is symmetric, which shows that (331) and (111) kinks are equal in energy. We have shown that an asymmetric polar-step free-energy plot can indeed produce an island with a symmetry axis at a distance d from the Wulff point, if the free energy $f(\phi)$ satisfies $f(\pi-\phi)=f(\phi)+2d\cos(\phi)$ for every angle ϕ.

We have calculated the step free energy with the two-dimensional Ising model, where fluctuations of steps are allowed both parallel and perpendicular to the missing-row direction, and we have considered two approximations to the step free energy, based on a one-dimensional solid-on-solid model. One model considers only step fluctuations perpendicular to the MR's, while the other allows only step fluctuations perpendicular to the MR's. Due to the low formation energy of parallel fluctuations, $f_{\parallel}$ provides the best approximation to the step free energy for most step orientations. Only steps very close to the perfect MR orientation are better described by $f_{\perp}$.

The second, stable type of island that we considered, has only (111)-type steps. For these islands, the Wulff construction is symmetric. It is obtained by using only the (111) part of the full construction and mirroring it with respect to the axis parallel to the MR direction, through the Wulff point. As a function of temperature, the aspect ratio of these almond-shaped islands first decreases, before it diverges at the roughening temperature.

Monte Carlo calculations of the step free energy were performed, in which both parallel and perpendicular fluctuations were allowed, like in the Ising model. At each temperature the MC results accurately reproduce the results of the Ising model and follow the inner contour of the two energy curves, $f_{\parallel}$ and $f_{\perp}$, obtained analytically for the parallel and perpendicular fluctuation approximations.

ACKNOWLEDGMENTS

This work is part of the research program of the ''Stichting voor Fundamenteel Onderzoek der Materie'' (FOM) and is financially supported by the ''Nederlandse Organisatie voor Wetenschappelijk Onderzoek'' (NWO).

APPENDIX: MONTE CARLO SIMULATION

We used a Monte Carlo simulation for calculating the step free energy as a function of temperature and orientation, allowing all steps to have excursions parallel and perpendicular to the MR direction. An example of such a step is shown in Fig. 7(a). It consists of step segments in all four directions. In the simulations, such configurations were generated for long step sections, typically a few hundred lattice constants, for each orientation, according to the Metropolis algorithm.[44] To calculate the free energy of the step, it is enough to count the number of occurrences N_{E_i} of just one of the possible energy states E_i, for which the number of different configurations C_{E_i} is known. The total free energy F of the step is then

$$F = E_i + kT\ln(N_{E_i}) - kT\ln(C_{E_i}) - kT\ln(N_{tot}), \quad \text{(A1)}$$

where N_{tot} is the total number of step configurations generated in the simulation. It is straightforward to calculate the total number of configurations with r-step segments to the right, zero-step segments to the left, u-step segments upward,

and d-step segments downward. First choose p places [$1 \leqslant p \leqslant \min(d,r+1)$ if $d>0$ and $u=0$; $1 \leqslant p \leqslant \min(d,r)$ if $d>0$ and $u>0$; $p=0$ if $d=0$] between the r horizontal step segments where the step goes downward. These places can be chosen in

$$\binom{r+1}{p}$$

ways. We have to distribute the d downward step segments over these p places in such a way that on every place there is at least one downward step segment. There are

$$\binom{d-1}{p-1}$$

possibilities to distribute them, except for the case $p=d=0$. Finally, there are $r+1-p$ places left for the upward step segments, which gives

$$\binom{r-p+u}{u}$$

possibilities, except for the case $r-p+1=u=0$. So the total number of configurations with r step segments to the right, zero step segments to the left, u step segments upward, and d step segments downward is

$$C=\sum_{p=0}^{\min(d,r)} \binom{r+1}{p}\binom{d-1}{p-1}\binom{r-p+u}{u}. \tag{A2}$$

The simulation allows for both perpendicular and parallel fluctuations, but the step configurations which are counted all have the same fluctuation direction. It is now possible to predict which step formation energy will occur most frequently and can best be counted during the simulation. The number of times that a configuration with energy E_i occurs during the simulation is proportional to

$$N_{E_i} \propto C_{E_i} e^{-E_i/kT}. \tag{A3}$$

In this way it becomes possible to efficiently calculate the free energy of long step sections, of, e.g., 600 lattice constants. This is important, because a step of finite length has a free energy per unit length, which is higher than that for an infinitely long step with the same overall orientation, which introduces a modest finite-size effect, as is visible in the lower inset of Fig. 12.

[1] G. Wulff, Z. Kristallogr. **34**, 449 (1901).

[2] C. Herring, Phys. Rev. **82**, 87 (1951).

[3] P. Stolze, J. Phys.: Condens. Matter **6**, 9495 (1994).

[4] L.D. Landau and E.M. Lifschitz, *Statistical Mechanics* (Pergamon, Oxford, 1980), Vol. I.

[5] A.F. Andreev, Zh. Éksp. Teor. Fiz. **80**, 2042 (1981) [Sov. Phys. JETP **53**, 1063 (1981)].

[6] T. Michely and G. Comsa, Surf. Sci. **256**, 217 (1991).

[7] M.J. Rost, T. Michely, and G. Comsa, Phys. Rev. B **57**, 1992 (1998).

[8] H.P. Bonzel and A. Emundts, Phys. Rev. Lett. **84**, 5804 (2000).

[9] M.J. Rost, S.B. van Albada, and J.W.M. Frenken, Phys. Rev. Lett. **86**, 5938 (2001).

[10] B.S. Schwarzentruber, Y.-W. Mo, R. Kariotis, M.G. Lagally, and M.B. Webb, Phys. Rev. Lett. **65**, 1913 (1990).

[11] M.J. Rost, R. van Gastel, and J.W.M. Frenken, Phys. Rev. Lett. **84**, 1966 (2000).

[12] H. van Beijeren and I. Nolden, in *Structure and Dynamics of Surfaces II*, edited by W. Schommers and P. von Blanckenhagen, *Topics in Current Physics 2* (Springer-Verlag, Berlin, 1986).

[13] The islands observed in Ref. 9 are too small to be considered as the equilibrium shape obtained from a Wulff construction. However, from the fact that the (331) and (111) kinks are observed with precisely the same frequency in these small islands, we conclude that also the equilibrium shape in the thermodynamic limit, as can be calculated from a Wulff construction, must be symmetric.

[14] When the Wulff construction is applied, first, a line segment is drawn from the Wulff point to a point on the polar-step free-energy plot. From this point, a line is drawn perpendicular to the first one. The distance along this line between the point on the polar plot and the place where it touches the island contour is proportional to the derivative of the step free energy with respect to the angle of the step (Refs. 18 and 16). The derivative is zero in the extrema of the step free energy, so the island contour and the polar plot coincide in these points.

[15] M.J. Rost, S.B. van Albada, and J.W.M. Frenken (unpublished).

[16] C. Rottman and M. Wortis, Phys. Rev. B **24**, 6274 (1981).

[17] J.E. Avron, H. van Beijeren, L.S. Schulman, and R.K.P. Zia, J. Phys. A **15**, L81 (1982).

[18] W.K. Burton, N. Cabrera, and F.C. Frank, Philos. Trans. R. Soc. London, Ser. A **243**, 299 (1951).

[19] E. Carlon and H. van Beijeren, Phys. Rev. Lett. **76**, 4191 (1996).

[20] M. Sturmat, R. Koch, and K.H. Rieder, Phys. Rev. Lett. **77**, 5071 (1996).

[21] M.J. Rost and J.W.M. Frenken, Phys. Rev. Lett. **87**, 039603 (2001).

[22] L. Kuipers, M.S. Hoogeman, and J.W.M. Frenken, Phys. Rev. B **52**, 11 387 (1995).

[23] M.S. Hoogeman, L. Kuipers, D.C. Schlösser, and J.W.M. Frenken, Surf. Sci. **447**, 25 (2000).

[24] R.K.P. Zia and J.E. Avron, Phys. Rev. B **25**, 2042 (1985).

[25] There is one detail which we neglect when using the two-dimensional Ising model on a MRR surface: the Ising model does not take into account the fact that each adatom and vacancy cluster can also exist with its (111) and (331) sides interchanged. For most clusters this is no problem, because the only clusters that contribute to the step free energy are those which intersect

the step. By neglecting the mirrored adatom and vacancy clusters at the step, we slightly underestimate the step free energy in our version of the Ising model.
[26] J.M. Kosterlitz and D.J. Thouless, J. Phys. C **6**, 1181 (1973).
[27] D. Wolf, H. Jagodzinski, and W. Moritz, Surf. Sci. **77**, 283 (1978).
[28] P. Bak, Solid State Commun. **32**, 581 (1979).
[29] J.C. Campuzano, M.S. Foster, G. Jennings, R.F. Willis, and W. Unertl, Phys. Rev. Lett. **54**, 2684 (1985).
[30] J. Villain and I. Vilfan, Surf. Sci. **199**, 165 (1988).
[31] I. Vilfan and J. Villain, Surf. Sci. **257**, 368 (1991).
[32] M. den Nijs, Phys. Rev. Lett. **66**, 907 (1991).
[33] J. Sprösser, B. Salanon, and J. Lapujoulade, Europhys. Lett. **16**, 283 (1991).
[34] U. Romahn, P. von Blanckenhagen, C. Kroll, and W. Göpel, Phys. Rev. B **47**, 12 840 (1993).
[35] G. Mazzeo, G. Jug, A.C. Levi, and E. Tossati, Surf. Sci. **273**, 237 (1992).
[36] L. Barbier, B. Salanon, and J. Sprösser, Surf. Rev. Lett. **1**, 75 (1994).
[37] K. Rommelse and M. den Nijs, Phys. Rev. Lett. **59**, 2578 (1987).
[38] G. Gallavotti, Commun. Math. Phys. **27**, 103 (1972).
[39] D.B. Abraham and P. Reed, Phys. Rev. Lett. **33**, 377 (1974).
[40] D.B. Abraham and P. Reed, Commun. Math. Phys. **49**, 35 (1976).
[41] M. Aizenmann, Commun. Math. Phys. **73**, 83 (1980).
[42] E.G. McRae, T.M. Buck, R.A. Malic, and G.H. Wheatley, Phys. Rev. B **36**, 2341 (1987).
[43] D.T. Keane, P.A. Bancel, J.L. Jordan-Sweet, G.A. Held, A. Mak, and R.J. Birgeneau, Surf. Sci. **250**, 8 (1991).
[44] M. Newman and G. Barkema, *Monte Carlo Methods in Statistical Physics* (Oxford University Press, Oxford, 1999).